Electronic Supplementary Material (ESI) for RSC Advances.
This journal is © The Royal Society of Chemistry 2019

Supplementary Material for

Dual-doped hierarchical porous carbon derived from biomass for advanced supercapacitors and lithium ion batteries

Wenjie Fan, [‡a] Hao Zhang, [‡a] Huanlei Wang*[a], Xiaochen Zhao, [b] Shijiao Sun, [c] Jing Shi, [a] Minghua Huang, [a] Wei Liu, [a] Yulong Zheng, [a] and Ping Li [a]

[a] *School of Materials Science and Engineering, Ocean University of China, Qingdao 266100, People's Republic of China*

[b] *College of Marine Science and Biological Engineering, Qingdao University of Science and Technology, Qingdao, 266042, People's Republic of China*

[c] *College of Materials Science and Engineering, Nanjing Tech University, Nanjing 210009, People's Republic of China*

‡ These authors contribute equally to this work.

*Corresponding authors.

Email: huanleiwang@gmail.com; huanleiwang@ouc.edu.cn

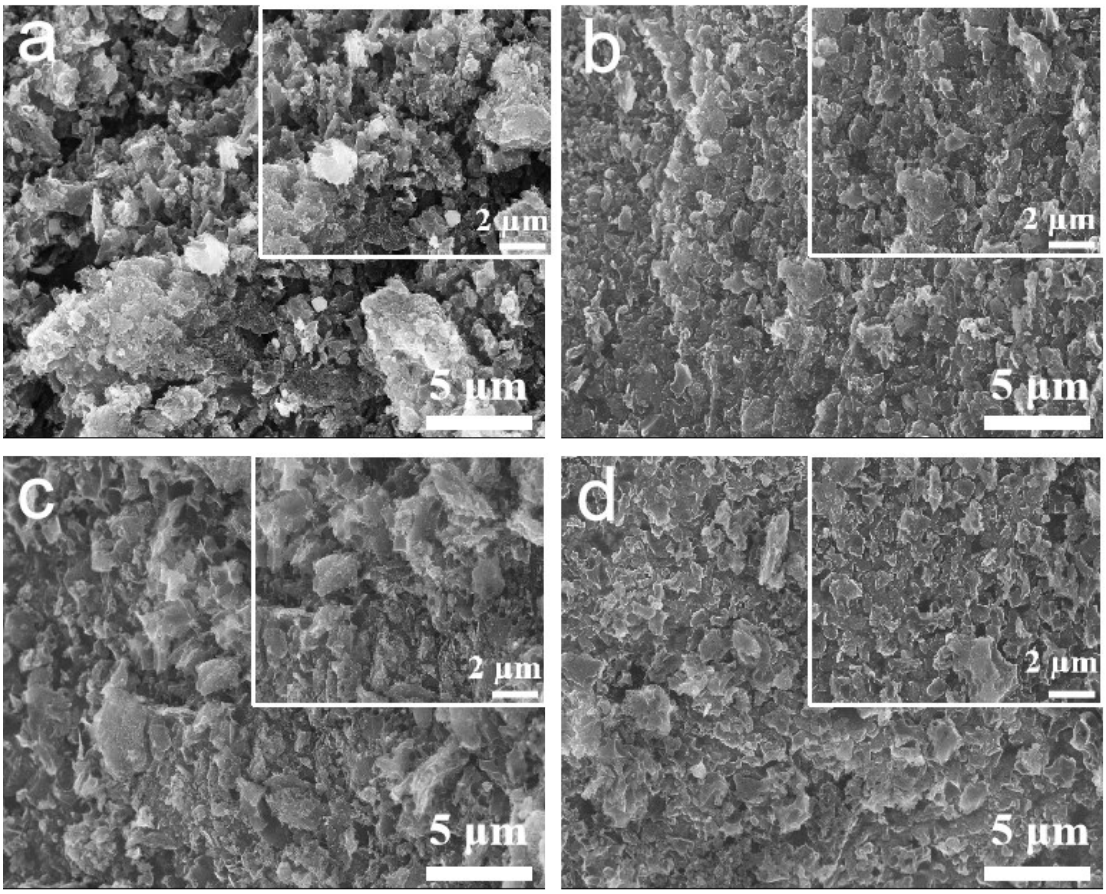

Fig. S1 SEM micrographs of (a) NLDPC-700-4-2, (b) NLDPC-900-4-2, (c) NLDPC-800-4-1, and (d) NLDPC-800-4-3.

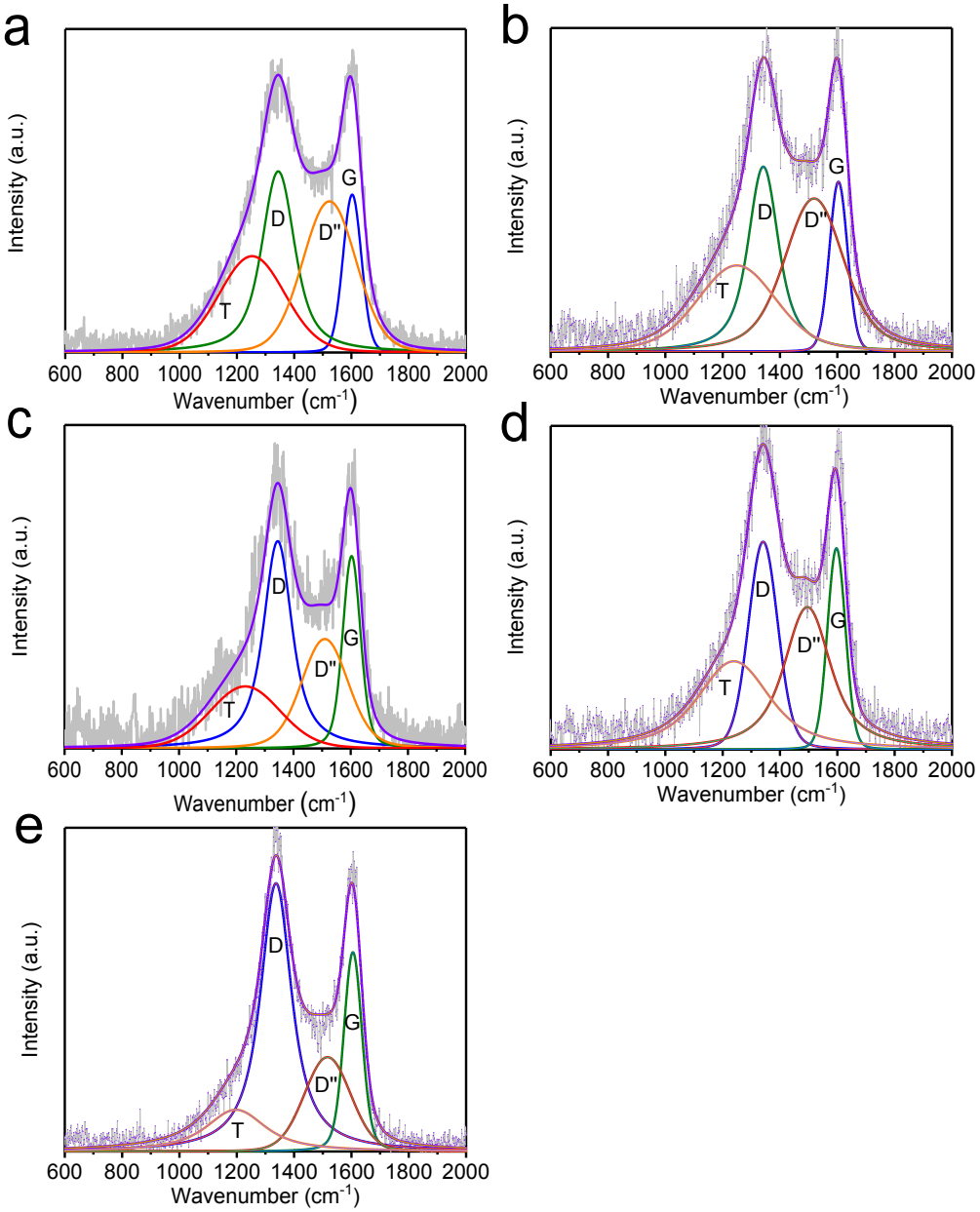

Fig. S2 Fitted Raman spectra of (a) NLDPC-700-4-2, (b) NLDPC-800-4-2, (c) NLDPC-900-4-2, (d) NLDPC-800-4-1, and (e) NLDPC-800-4-3 by using Voigt function.

Table S1 Peak characteristics of the D- and G-band of the Raman spectra.

Sample		Position (cm^{-1})	FWHM (cm^{-1})	I_D/I_G
NLDPC-700-4-2	D-mode	1344	136	2.54
	G-mode	1603	76	
NLDPC-800-4-2	D-mode	1342	126	2.32
	G-mode	1604	74	
NLDPC-900-4-2	D-mode	1345	119	2.10
	G-mode	1603	73	
NLDPC-800-4-1	D-mode	1341	121	1.72
	G-mode	1597	74	
NLDPC-800-4-3	D-mode	1337	130	2.88
	G-mode	1605	74	

Table S2 Relative surface concentrations (%) of nitrogen and oxygen species obtained by fitting N1s and O1s core level XPS spectra.

Sample	N-6	N-5	N-Q	N-X	O-I	O-II	O-III
NLDPC-700-4-2	28.95	29.79	22.19	19.07	6.04	54.06	39.90
NLDPC-800-4-2	21.39	23.28	33.11	22.22	4.64	61.99	33.37
NLDPC-900-4-2	10.57	14.57	49.42	25.44	2.52	44.11	53.36
NLDPC-800-4-1	23.66	42.66	18.68	15.00	1.60	63.62	34.78
NLDPC-800-4-3	14.55	16.47	41.71	27.27	2.85	82.87	14.28

Table S3 Absolute surface concentrations (%) of nitrogen species obtained by fitting N1s core level XPS spectra.

Samples	N-6	N-5	N-Q	N-X
NLDPC-700-4-2	1.59	1.64	1.22	1.05
NLDPC-800-4-2	0.70	0.76	1.08	0.73
NLDPC-900-4-2	0.24	0.34	1.14	0.59
NLDPC-800-4-1	0.95	1.72	0.75	0.60
NLDPC-800-4-3	0.16	0.19	0.47	0.31

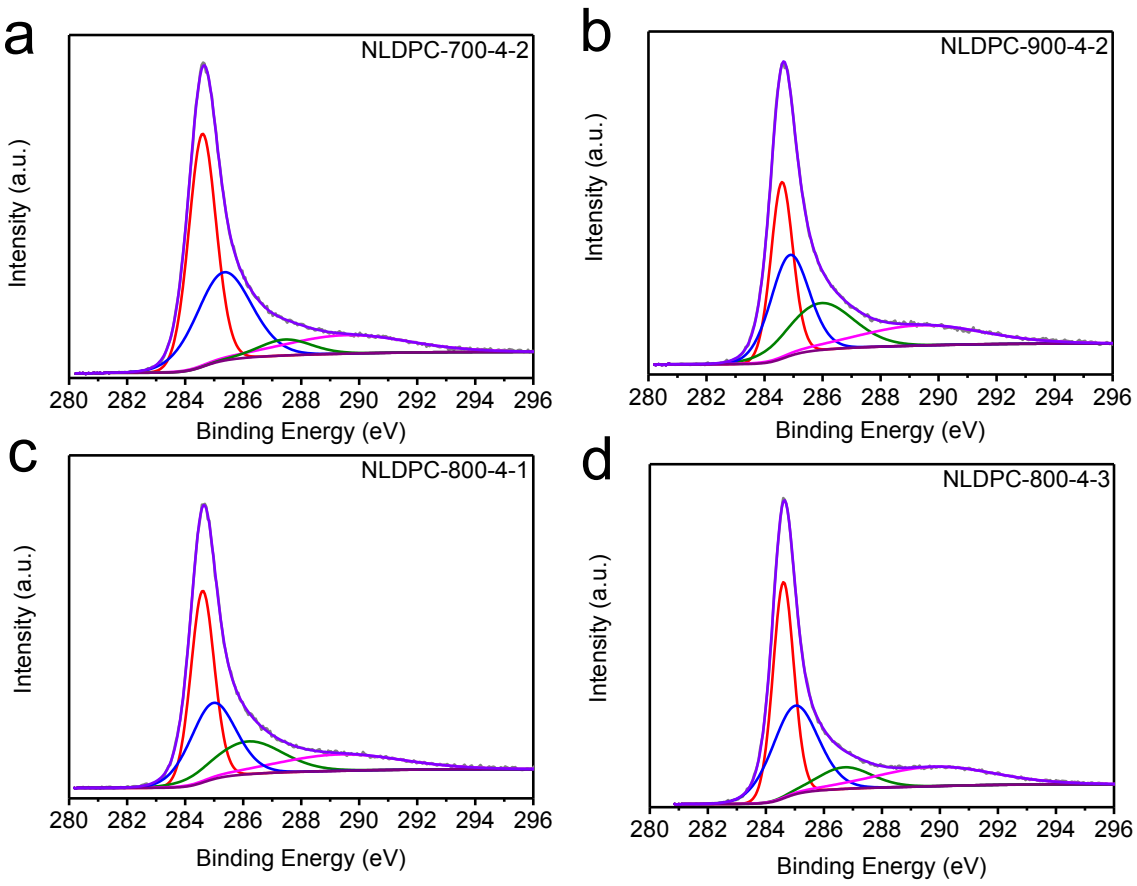

Fig. S3 High-resolution XPS C1s spectra of (a) NLDPC-700-4-2, (b) NLDPC-900-4-2, (c) NLDPC-800-4-1, and (d) NLDPC-800-4-3.

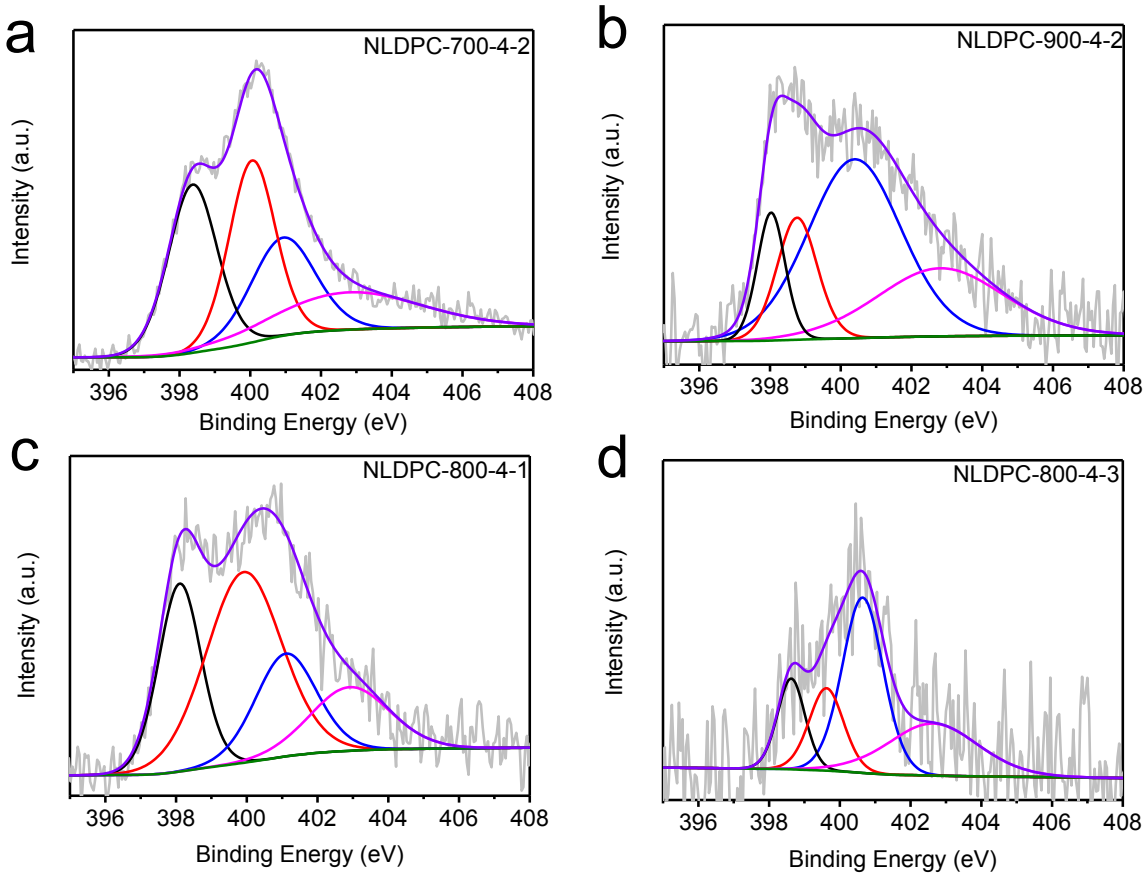

Fig. S4 High-resolution XPS N1s spectra of (a) NLDPC-700-4-2, (b) NLDPC-900-4-2, (c) NLDPC-800-4-1, and (d) NLDPC-800-4-3.

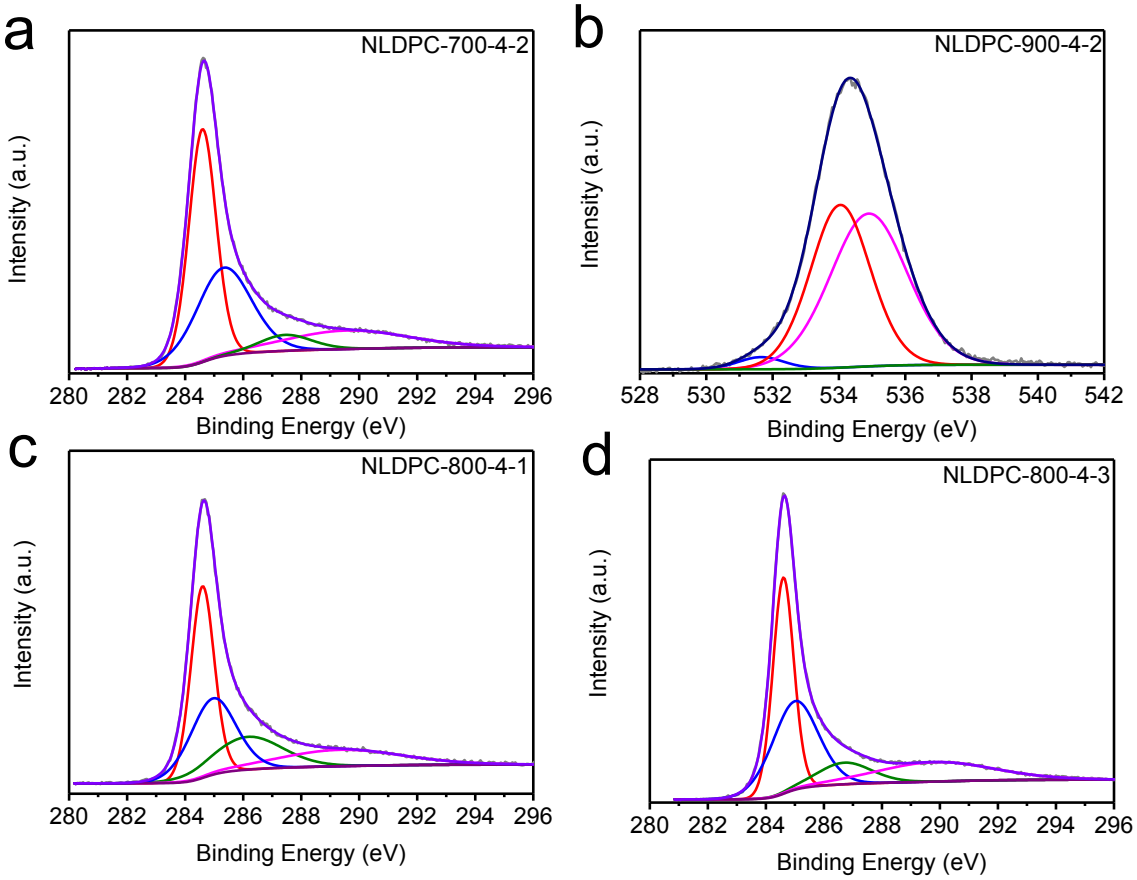

Fig. S5 High-resolution XPS O1s spectra of (a) NLDPC-700-4-2, (b) NLDPC-900-4-2, (c) NLDPC-800-4-1, and (d) NLDPC-800-4-3.

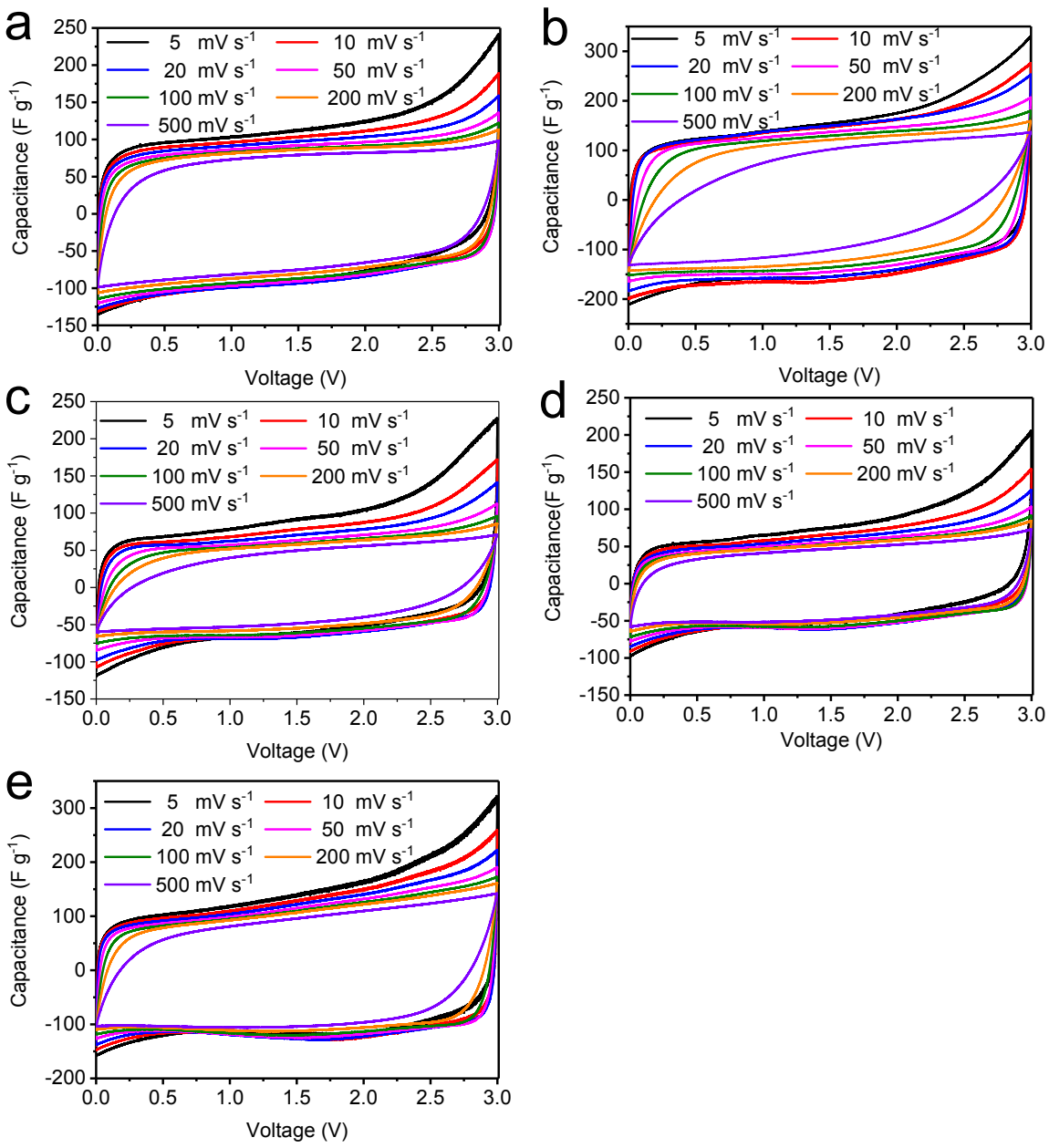

Fig. S6 CV curves of (a) NLDPC-700-4-2, (b) NLDPC-800-4-2, (c) NLDPC-900-4-2, (d) NLDPC-800-4-1, and (e) NLDPC-800-4-3 at different scan rates.

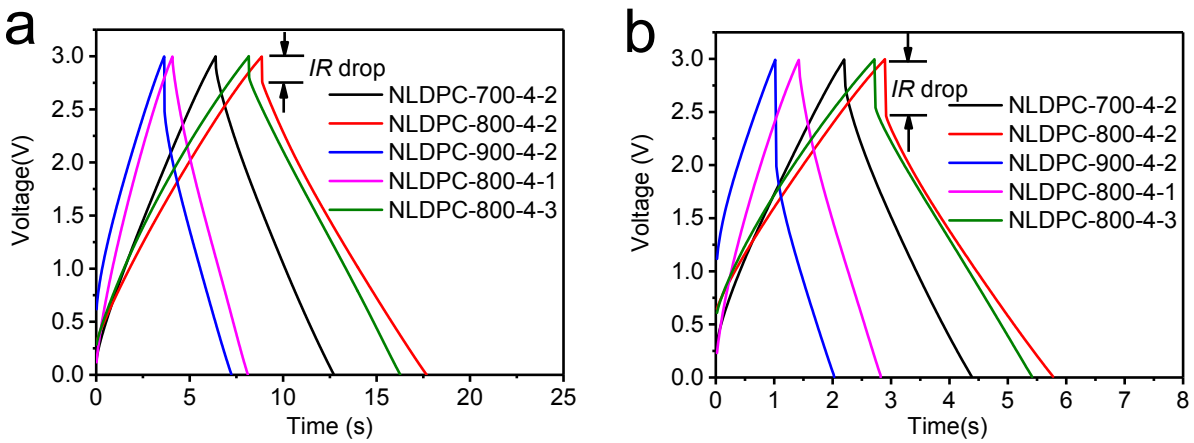

Fig. S7 Galvanostatic charge-discharge profiles of NLDPC samples tested at (a) 20 A g^{-1}, and (b) 50 A g^{-1}.

Table S4 Comparison of capacitance and energy density of carbon-based electrodes for supercapacitors.

Sample	Electrolyte (Voltage range)	Capacitance	Capacitance retention (%)	Cyclability	Energy
NLDPC-800-4-2 (this work)	EMIM BF_4 (0-3 V)	163 F g^{-1} at 0.5 A g^{-1} 110 F g^{-1} at 100 A g^{-1}	68 (0.5-100 A g^{-1})	92% after 10 000 cycles（10 A g^{-1}）	50 W h kg^{-1} at 373 W kg^{-1} 21 W h kg^{-1} at 40 kW kg^{-1}
Activated porous carbon sphere[1]	TEA BF_4/AN (0-2 V)	111 F g^{-1} at 1 A g^{-1} 90 F g^{-1} at 10 A g^{-1}	81 (1-10 A g^{-1})	-	-
	EMIM BF_4 (0-3 V)	170 F g^{-1} at 1 A g^{-1} 86 F g^{-1} at 10 A g^{-1}	51 (1-10 A g^{-1})	-	-
Bimodal micro-mesoporous carbons[2]	EMIM BF_4 (0-3 V)	-	75 (0.1-30 A g^{-1})	90% after 4 000 cycles（10 A g^{-1}）	21.5 W h kg^{-1} at 19 kW kg^{-1}
	EMIM BF_4/AN (0-3 V)	-	78 (0.1-50 A g^{-1})	98% after 1 000 cycles（10 A g^{-1}）	25 W h kg^{-1} at 19 kW kg^{-1}
Carbon nanotubes[3]	EMIM BF_4 (0-3 V)	144 F g^{-1} at 5 mV s^{-1}	-	-	45 W h kg^{-1} at 4.0 kW kg^{-1}
	BMIM BF_4 (0-3 V)	150 F g^{-1} at 5 mV s^{-1}	-	-	47 W h kg^{-1} at 4.3 kW kg^{-1}
C/C composites[4]	TEA BF_4/PC (0-3 V)	140 F g^{-1} at 0.05 A g^{-1} 92.1 F g^{-1} at 10 Ag^{-1}	66 (0.05-10 A g^{-1})	82.1% after 10 000 cycles (2.5 A g^{-1})	43.7 W h kg^{-1}
	EMIM BF_4 (0-3.5 V)	156 F g^{-1} at 0.05 A g^{-1} 95 F g^{-1} at 10 Ag^{-1}	61 (0.05-10 A g^{-1})	91.9% after 5 000 cycles (2.5 A g^{-1})	66.3 W h kg^{-1} at 43.7 W kg^{-1} 40.5 W h kg^{-1} at 8750 W kg^{-1}
Carbon nanosheet framework[5]	EMIM BF_4 (0-3.5 V)	-	50.7 (1-20 A g^{-1})	88.5% after 5 000 cycles (3 A g^{-1})	60.4 W h kg^{-1} at 1.75 kW kg^{-1}

Mesoporous activated carbon[6]	EMIM BF_4 (0-3.5 V)	188 F g^{-1} at 1 A g^{-1}	-	-	80 W h kg^{-1} at 870 W kg^{-1}
High-temperature synthesis graphene[7]	EMIM BF_4 (0-3.5 V)	172 F g^{-1} at 2 A g^{-1} 125 F g^{-1} at 100 A g^{-1}	73 (2-100 A g^{-1})	90% after 100 000 cycles (100 A g^{-1})	73 W h kg^{-1} at 3.5 kW kg^{-1} 53 W h kg^{-1} at 175 kW kg^{-1}
	EMIM BF_4 (0-4 V)	192 F g^{-1} at 5 A g^{-1} 148 F g^{-1} at 100 A g^{-1}	77 (5-100 A g^{-1})	81% after 80 000 cycles (100 A g^{-1})	106 W h kg^{-1} at 10 kW kg^{-1} 82 W h kg^{-1} at 200 kW kg^{-1}
	EMIM TFSI (0-3.5 V)	190 F g^{-1} at 2 A g^{-1} 143 F g^{-1} at 100 A g^{-1}	74 (2-100 A g^{-1})	89% after 10 000 cycles (100 A g^{-1})	81 W h kg^{-1} at 3.5 kW kg^{-1} 61 W h kg^{-1} at 175 kW kg^{-1}
	EMIM TFSI (0-4 V)	244 F g^{-1} at 5 A g^{-1} 173 F g^{-1} at 100 A g^{-1}	71 (5-100 A g^{-1})	70% after 10 000 cycles (100 A g^{-1})	135 W h kg^{-1} at 10 kW kg^{-1} 96 W h kg^{-1} at 200 kW kg^{-1}
RGO-IL-MNCNTs[8]	EMIM BF_4 (-2.3-1.7 V)	201.6 F g^{-1} at 0.1 Ag^{-1}	-	93.6% after 10 000 cycles (2 A g^{-1})	131.8 W h kg^{-1} at 892.6 W kg^{-1}
Graphene /activated carbon hydrogel[9]	EMIM BF_4 (0-3 V)	116.6 F g^{-1} at 1 Ag^{-1}	-	74.4% after 20 000 cycles (10 A g^{-1})	36.4 W h kg^{-1} at 633.7 W kg^{-1}
Corncob derived activated porous carbon[10]	EMIM TFSI (0-3 V)	35 F g^{-1} at 0.1 A g^{-1}	-	-	-
	EMIM PF_6 (0-3 V)	45 F g^{-1} at 0.1 A g^{-1}	-	-	-
	EMIM BF_4 (0-3 V)	80 F g^{-1} at 0.1 A g^{-1}	-	50% after 500 cycles (0.1 A g^{-1})	25 W h kg^{-1} at 174 W kg^{-1}
Carbide-derived carbon[11]	EMIM BF_4 (0-3 V)	129 F g^{-1} at 0.1 A g^{-1}	-	-	-

High-mesopore-volume nanocarbons[12]	TEA BF_4/PC (0-2.7 V)	180 F g^{-1} at 0.5 A g^{-1} 157 F g^{-1} at 10 A g^{-1}	87 (0.5-10 A g^{-1})	84% after 10 000 cycles (5 A g^{-1})	38 W h kg^{-1} at 574 W kg^{-1} 21 W h kg^{-1} at 11.5 kW kg^{-1}
	EMIM BF_4 (0-3.5 V)	215 F g^{-1} at 0.5 A g^{-1} 148 F g^{-1} at 10 A g^{-1}	69 (0.5-10 A g^{-1})	-	76 W h kg^{-1} at 744 W kg^{-1} 34 W h kg^{-1} at 14.9 kW kg^{-1}
rGO[13]	SET_3 TFSI (0-2.5 V)	95.8 F g^{-1} at 5 mV s^{-1} 80 F g^{-1} at 30 mV s^{-1}	84 (5-30 mV s^{-1})	-	-
	SET_3 TFSI/GO (0-2.5 V)	125.3 F g^{-1} at 5 mV s^{-1} 110.6 F g^{-1} at 30 mV s^{-1}	88 (5-30 mV s^{-1})	65% after 3 000 cycles (1.5 A g^{-1})	17.7 W h kg^{-1} at 875 W kg^{-1}
Carbon nanosphere[14]	EMI BF_4 (0-3.4 V)	156 F g^{-1} at 2 mV s^{-1} 88 F g^{-1} at 100 mV s^{-1}	56 (2-100 mV s^{-1})	-	-
Coarse-grained carbide derived carbon[15]	NET_4 BF_4/AN (0-2.5 V)	134 F g^{-1} at 2 mV s^{-1} 100 F g^{-1} at 250 mV	75 (2-250 mV s^{-1})	-	-
Mesoporous carbon[16]	Nafion (1-2.5 V)	134.73 F g^{-1} at 0.18 A g^{-1} 118.29 F g^{-1} at 1.8 A g^{-1}	88 (0.18-1.8A g^{-1})	-	33.79 W h kg^{-1} at 1.03 kW kg^{-1}
Ordered mesoporous carbon[17]	EMIM BF_4 (-2-2 V)	186 F g^{-1} at 0.25 A g^{-1} 140 F g^{-1} at 20 A g^{-1}	75 (0.25-20 A g^{-1})	93% after 5 000 cycles (2 A g^{-1})	-
N-doped mesoporous carbon[18]	TEA BF_4/AN (0-3 V)	111 F g^{-1} at 0.5 A g^{-1} 96 F g^{-1} at 10 A g^{-1}	86 (0.5-10 A g^{-1})	92% after 5 000 cycles (10 A g^{-1})	35 W h kg^{-1} at 411 W kg^{-1} 21 W h kg^{-1} at 12 kW kg^{-1}
Hierarchical porous carbon[19]	EMI BF_4 (0-3.5 V)	141 F g^{-1} at 1 A g^{-1} 105 F g^{-1} at 80 A g^{-1}	74 (1-80 A g^{-1})	93% after 10 000 cycles (10 A g^{-1})	59.8 W h kg^{-1} at 875 W kg^{-1} 44.7 W h kg^{-1} at 73.1 kW kg^{-1}

Ionic liquid modified reduced graphene oxide[20]	EMIM BF_4 (0-3.5 V)	135 F g^{-1} at 0.5 A g^{-1} 114 F g^{-1} at 20 A g^{-1}	85 (0.5-20 A g^{-1})	92% after 2 000 cycles (10 A g^{-1})	49 W h kg^{-1} at 18 kW kg^{-1}

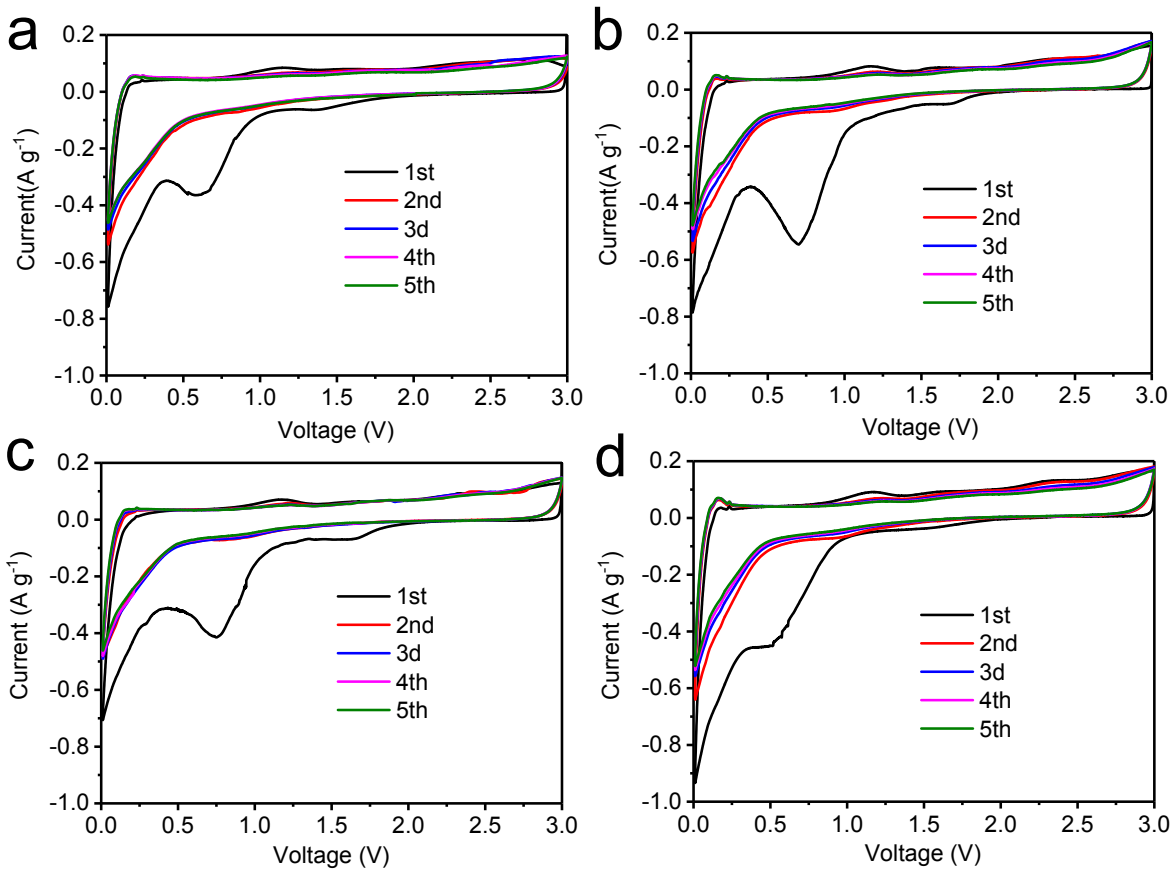

Fig. S8 CV curves of (a) NLDPC-700-4-2, (b) NLDPC-900-4-2, (c) NLDPC-800-4-1, and (d) NLDPC-800-4-3 at 0.1 mV s^{-1}.

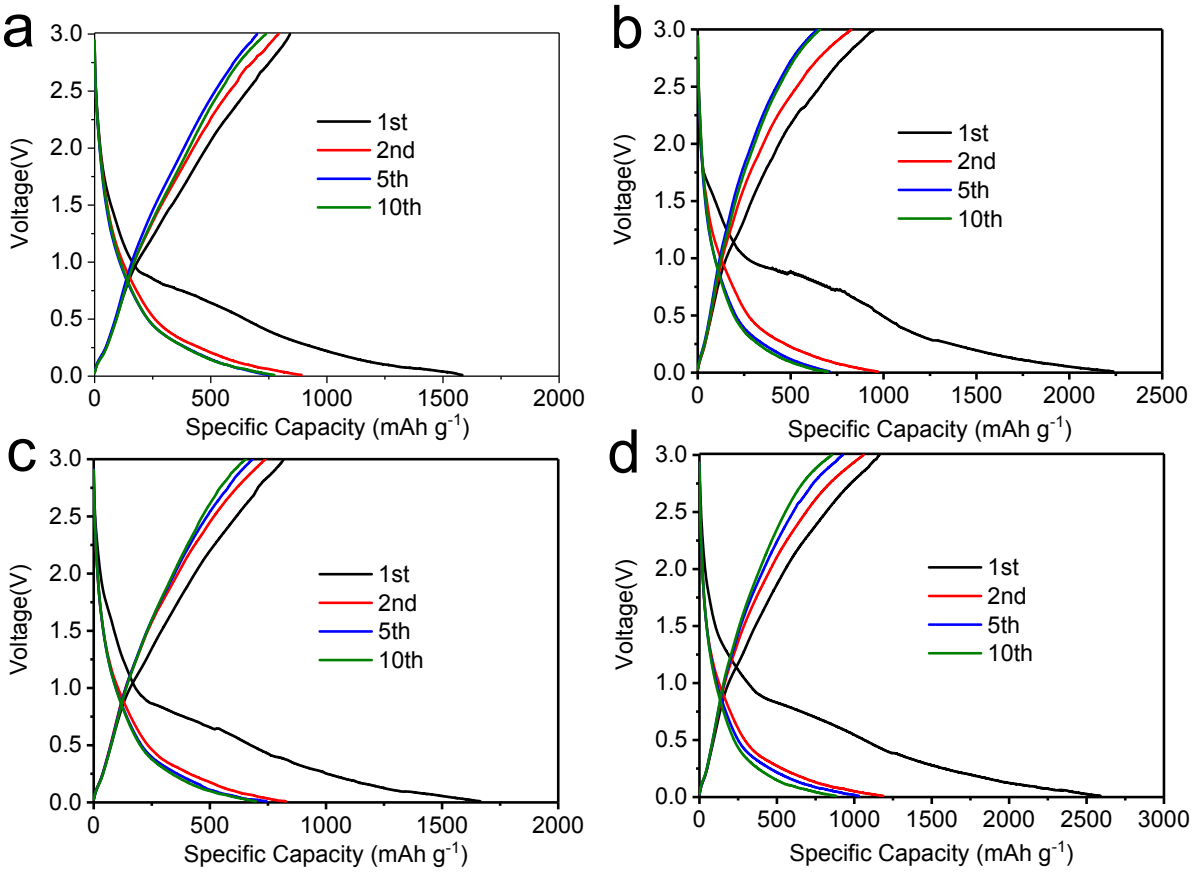

Fig. S9 Charge-discharge curves of (a) NLDPC-700-4-2, (b) NLDPC-900-4-2, (c) NLDPC-800-4-1, and (d) NLDPC-800-4-3 at 0.1 A g^{-1}.

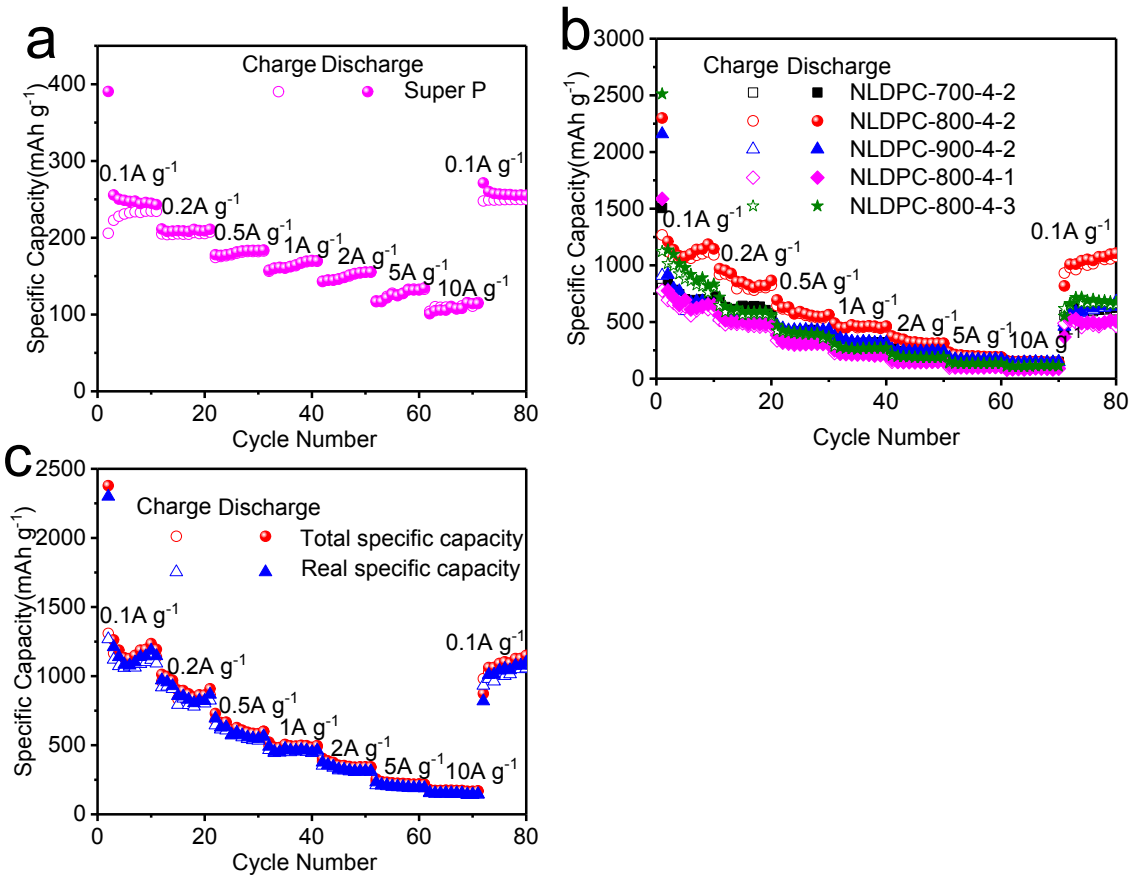

Fig. S10 (a)Rate capability at different current densities of super P. (b) The real specific capacity of NLDPCs sample at different current densities.(c) The total specific capacity and real specific capacity of NLDPC-800-4-2 sample at different current densities.

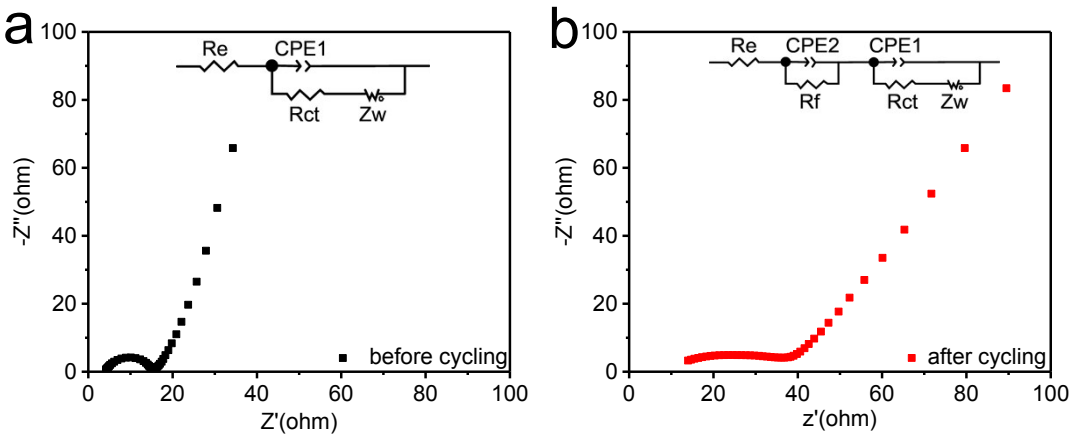

Fig. S11 The Nyquist plots for NLDPC-800-4-2 (a) before cycling and (b) after 500 cycles.

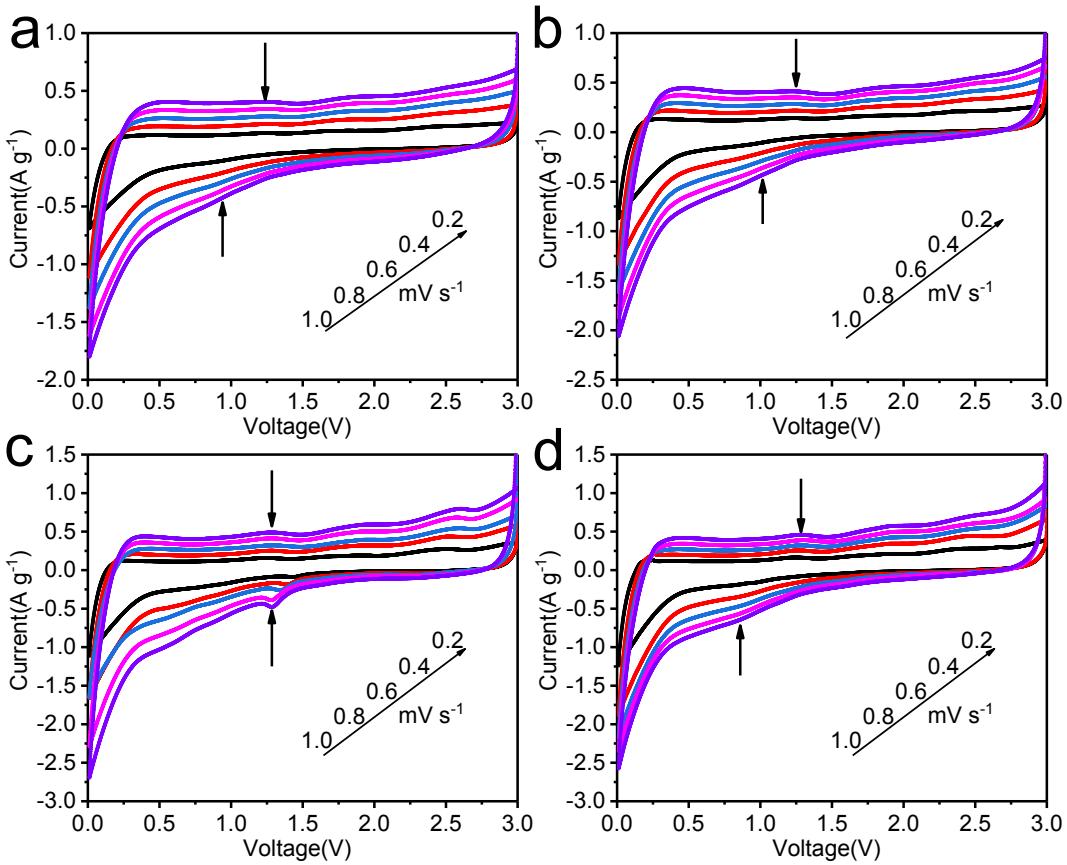

Fig. S12 CV curves at diffffferent scan rates of (a) NLDPC-700-4-2, (b) NLDPC-900-4-2, (c) NLDPC-800-4-1 and (d) NLDPC-800-4-3.

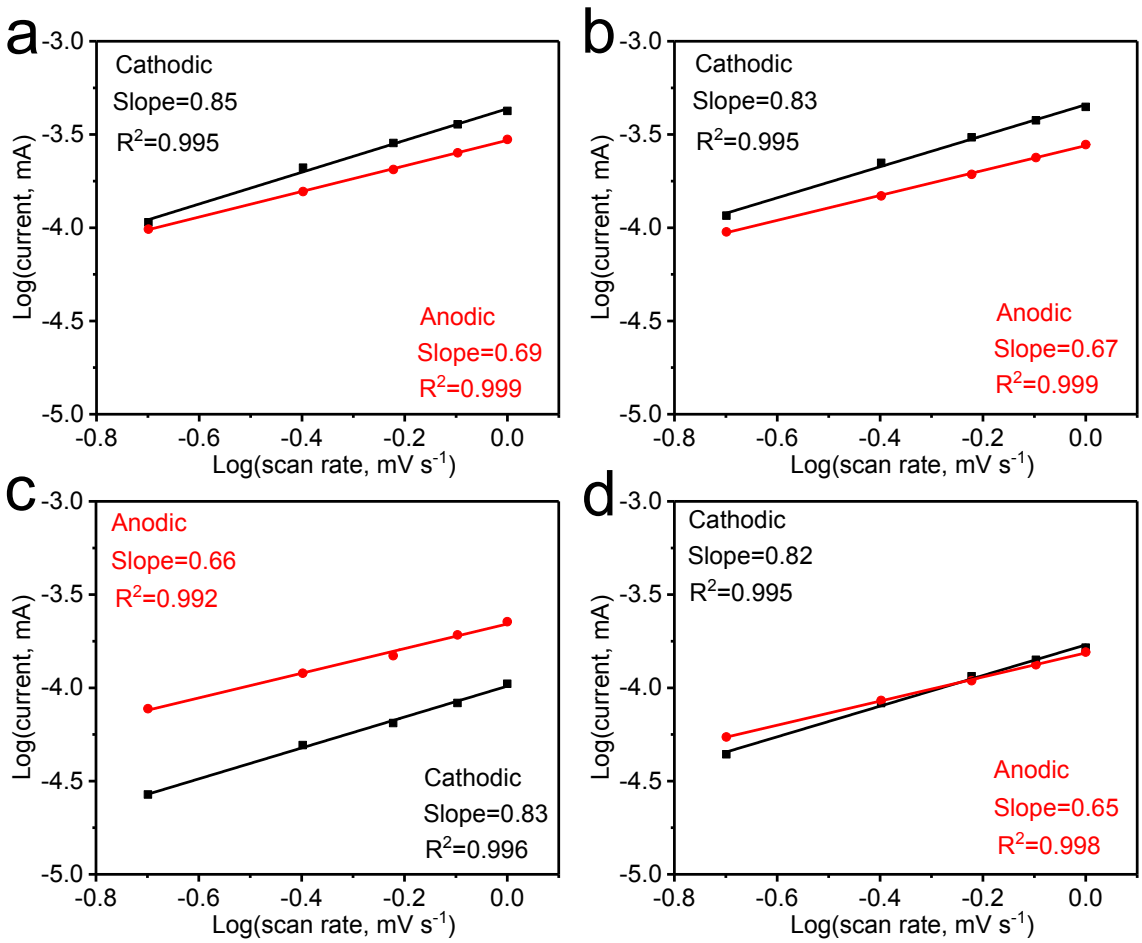

Fig. S13 Selected cathodic and anodic *b* values of peak currents (as indicated in Fig. S12) for (a) NLDPC-700-4-2, (b) NLDPC-900-4-2, (c) NLDPC-800-4-1 and (d) NLDPC-800-4-3.

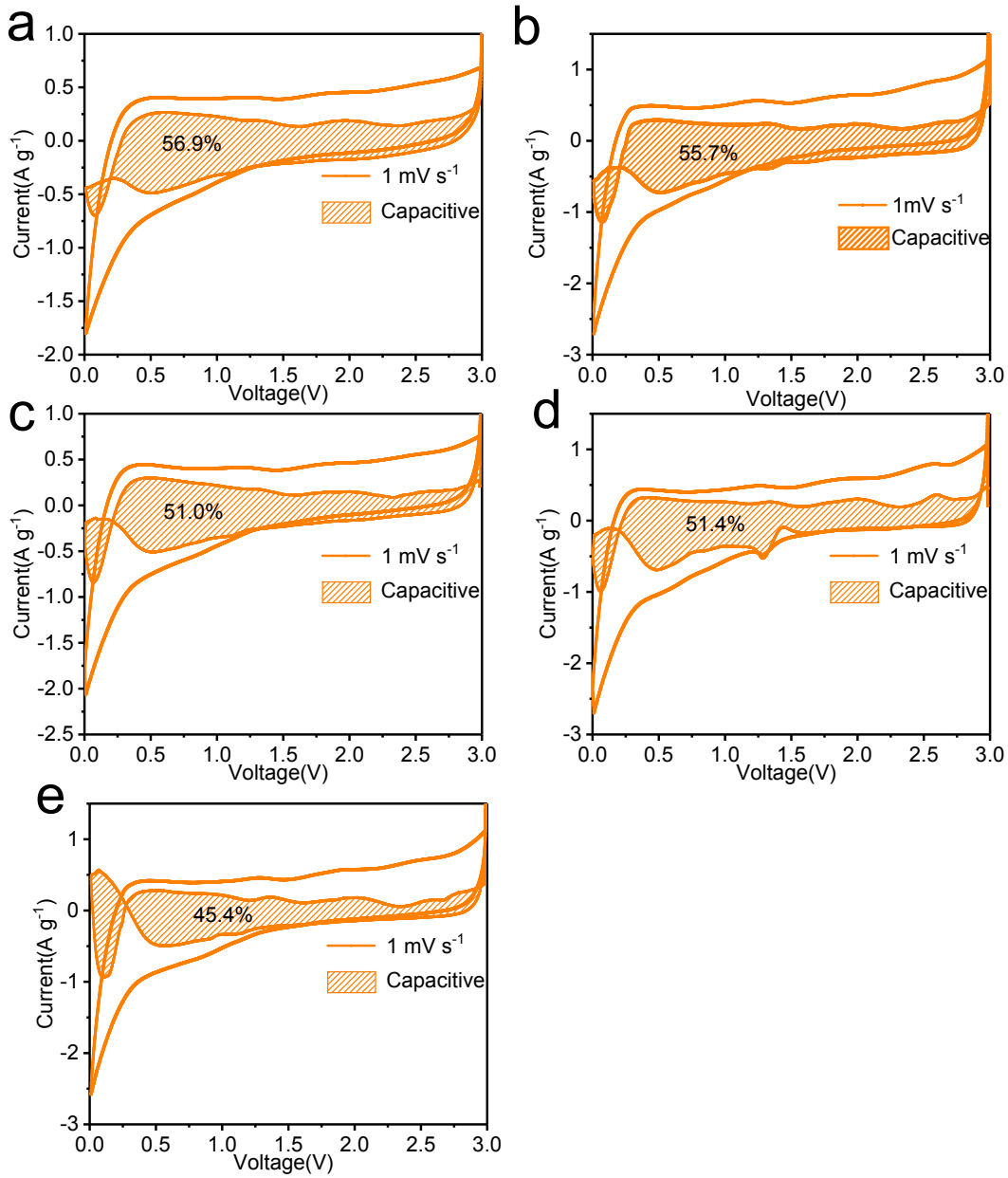

Fig. S14 The capacitive contribution of (a) NLDPC-700-4-2, (b) NLDPC-800-4-2,(c) NLDPC-900-4-2, (d) NLDPC-800-4-1 and (e) NLDPC-800-4-3 at a scan rate of 1 mV s^{-1}.

Table S5 Comparison of capacity of carbon-based electrodes for lithium-ion battery.

Sample	Electrolyte (Voltage range)	Initial coulombic efficiency (%)	Rate capacity	Cyclability
NLDPC-800-4-2 (this work)	1 M $LiPF_6$ (0.01-3V)	55.1	1262 mA h g^{-1} at 0.1 A g^{-1}; 730 mA h g^{-1} at 0.5 A g^{-1}; 256 mA h g^{-1} at 5 A g^{-1}; 178 mA h g^{-1} at 10 A g^{-1};	439 mA h g^{-1} after 500 cycles at 1 A g^{-1}
N/S co-doped carbon[21]	1 M $LiPF_6$ (0.01-3V)	75.6	1188 mA h g^{-1} at 0.1 A g^{-1}; 463 mA h g^{-1} at 5 A g^{-1};	653 mA h g^{-1} after 500 cycles at 1 A g^{-1}
Toast-like porous carbon[22]	1 M $LiPF_6$ (0.01-3V)-	35	1047 mA h g^{-1} at 0.1 A g^{-1}; 653 mA h g^{-1} at 0.5 A g^{-1}; 516 mA h g^{-1} at 1 A g^{-1};	730 mA h g^{-1} after 650 cycles at 1 A g^{-1}; 419 mA h g^{-1} after 1400 cycles at 4 A g^{-1}
Carbon nanosheet[23]	1 M $LiPF_6$ (0.01-3V)	50.	870.2 mA h g^{-1} at 0.05 A g^{-1}; 320 mA h g^{-1} at 10 A g^{-1}; 240 mA h g^{-1} at 20 A g^{-1};	1240 mA h g^{-1} after 125 cycles at 0.05 A g^{-1}; 415 mA h g^{-1} after 1300 cycles at 5 A g^{-1}
Ultrathin amorphous carbon nanosheet[4]	1 M $LiPF_6$ (0.01-3V)	59.4	731 mA h g^{-1} at 0.1 A g^{-1}; 447 mA h g^{-1} at 0.5 A g^{-1}; 315 mA h g^{-1} at 5 A g^{-1}; 283 mA h g^{-1} at 10 A g^{-1};	680 mA h g^{-1} after 700 cycles at 1 A g^{-1}; 579 mA h g^{-1} after 900 cycles at 2 A g^{-1}; 396 mA h g^{-1} after 900 cycles at 5 A g^{-1}
Phosphorous inside multi-walled carbon nanotube[24]	1 M $LiPF_6$ (0.01-3V)	-	446 mA h g^{-1} at 0.5 A g^{-1}; 361 mA h g^{-1} at 1 A g^{-1}; 246 mA h g^{-1} at 5 A g^{-1};	444 mA h g^{-1} after 500 cycles at 0.5 A g^{-1}
Nitrogen and halogen dual-doped porous carbon[25]	1 M $LiPF_6$ (0.01-3V)	54.2	664 mA h g^{-1} at 1 A g^{-1}; 456 mA h g^{-1} at 5 A g^{-1}	1010.3 mA h g^{-1} after 500 cycles at 1 A g^{-1}; 461 mA h g^{-1} after 800 cycles at 5 A g^{-1}
Hierarchical porous carbon microsphere[26]	1 M $LiPF_6$ (0.01-3V)	54.52	1140 mA h g^{-1} at 0.05 A g^{-1}; 467.6 mA h g^{-1} at 0.5 A g^{-1}; 232.9 mA h g^{-1} at 2 A g^{-1};	870 mA h g^{-1} after 120 cycles at 0.05 A g^{-1}

Hierarchical N-doped porous carbon[27]	1 M $LiPF_6$ (0.005-3V)	65.9	747 mA h g^{-1} at 0.05 A g^{-1}; 475 mA h g^{-1} at 0.4 A g^{-1}; 348 mA h g^{-1} at 1.6 A g^{-1};	740 mA h g^{-1} after 100 cycles at 0.05 A g^{-1}; 552 mA h g^{-1} after 450 cycles at 0.4 A g^{-1}
Hierarchically porous carbon[28]	1 M $LiPF_6$ (0.01-3V)	54.1	1200 mA h g^{-1} at 0.1 A g^{-1}; 750 mA h g^{-1} at 0.5 A g^{-1}; 300 mA h g^{-1} at 5 A g^{-1};	1200 mA h g^{-1} after 50 cycles at 0.1 A g^{-1}; 550 mA h g^{-1} after 500 cycles at 1 A g^{-1}; 370 mA h g^{-1} after 500 cycles at 5 A g^{-1}
Boron and nitrogen dual-doped 3D carbon nanofiber[29]	1 M $LiPF_6$ (0.02-3V)	-	1130 mA h g^{-1} at 0.1 A g^{-1}; 375 mA h g^{-1} at 5 A g^{-1}; 272 mA h g^{-1} at 10 A g^{-1}	Negligible capacity loss after 5000 cycles at 2 A g^{-1}
Nitrogen enriched spherical carbon particle[30]	1 M $LiPF_6$ (0.01-2.5V)	56	746 mA h g^{-1} at 0.1 A g^{-1}; 639 mA h g^{-1} at 0.5 A g^{-1};	820 mA h g^{-1} after 100 cycles at 0.1 A g^{-1}; 623 mA h g^{-1} after 500 cycles at 0.5 A g^{-1}
N/P dual-doped hollow carbon fibers/graphitic carbon nitride[31]	1 M $LiPF_6$ (0-3V)	55	1217 mA h g^{-1} at 0.1 A g^{-1}; 955 mA h g^{-1} at 0.5 A g^{-1}; 328 mA h g^{-1} at 10 A g^{-1};	1030 mA h g^{-1} after 1000 cycles at 1 A g^{-1}; 360 mA h g^{-1} after 4000 cycles at 10 A g^{-1}
Hard carbon nanoshell[32]	1 M $LiPF_6$ (0.01-3V)	53.4	1253 mA h g^{-1} at 0.1 A g^{-1}; 175 mA h g^{-1} at 20 A g^{-1};	1236 mA h g^{-1} after 100 cycles at 0.1 A g^{-1}
Nitrogen-deficient graphitic carbon nitride[33]	1 M $LiPF_6$ (0-3V)	45.7	860 mA h g^{-1} at 0.1 A g^{-1}; 359 mA h g^{-1} at 10 A g^{-1}; 328 mA h g^{-1} at 20 A g^{-1};	2753 mA h g^{-1} after 190 cycles at 0.1 A g^{-1}
Nitrogen-doped porous carbon[28]	1 M $LiPF_6$ (0.01-3V)	55.4	613 mA h g^{-1} at 0.5 A g^{-1}; 223 mA h g^{-1} at 5 A g^{-1}; 173 mA h g^{-1} at 10 A g^{-1}	300 mA h g^{-1} after 500 cycles at 2 A g^{-1}

Orderly meso-perforated spherical and apple-shaped 3D carbon[34]	1 M $LiPF_6$ (0.01-3V)	40	1072 mA h g^{-1} at 0.2 A g^{-1}; 772 mA h g^{-1} at 0.5 A g^{-1}; 276 mA h g^{-1} at 5 A g^{-1}	1716 mA h g^{-1} after 175 cycles at 0.2 A g^{-1}; 500 mA h g^{-1} after 500 cycles at 1 A g^{-1}
Carbon nanosheet[35]	1 M $LiPF_6$ (0.01-3V)	53.9	654 mA h g^{-1} at 0.1 A g^{-1}; 463 mA h g^{-1} at 0.5 A g^{-1}; 280 mA h g^{-1} at 5 A g^{-1}	600 mA h g^{-1} after 500 cycles at 1 A g^{-1}
Sandwich-like nanosheet[36]	1 M $LiPF_6$ (0.01-3V)	48.5	575.7 mA h g^{-1} at 0.1 A g^{-1}; 507.8 mA h g^{-1} at 0.5 A g^{-1};	643 mA h g^{-1} after 60 cycles at 0.1 A g^{-1}; 788.9 mA h g^{-1} after 500 cycles at 1 A g^{-1}; 406 mA h g^{-1} after 2700 cycles at 5 A g^{-1}
2D/3D carbon hybrids[37]	1 M $LiPF_6$ (0.005-3V)	-	775 mA h g^{-1} at 0.1 A g^{-1}; 527 mA h g^{-1} at 0.5 A g^{-1}; 241 mA h g^{-1} at 5 A g^{-1}	636 mA h g^{-1} after 160 cycles at 0.1 A g^{-1}; 365 mA h g^{-1} after 1000 cycles at 2 A g^{-1}
N, O-codoped hierarchical porous carbon[38]	1 M $LiPF_6$ (0.01-3V)	64	650 mA h g^{-1} at 0.5 A g^{-1}; 220 mA h g^{-1} at 5 A g^{-1}; 170 mA h g^{-1} at 10 A g^{-1};	350 mA h g^{-1} after 500 cycles at 2 A g^{-1}
Interconnected highly graphitic carbon nanaosheet[39]	1 M $LiPF_6$ (0-3V)	62.9	486.9 mA h g^{-1} at 0.5 C; 305 mA h g^{-1} at 5 C; 161.4 mA h g^{-1} at 10 C;	300.9 mA h g^{-1} after 500 cycles at 1 C; 215 mA h g^{-1} after 2000 cycles at 5 C; 139.6 mA h g^{-1} after 3000 cycles at 10 C

References

1. J. Tang, J. Wang, L. K. Shrestha, M. S. A. Hossain, Z. A. Alothman, Y. Yamauchi and K. Ariga, *ACS Appl. Mater. Interfaces*, 2017, **9**, 18986-18993.
2. M. Sevilla and A. B. Fuertes, *ChemSusChem*, 2016, **9**, 1880-1888.
3. H. M. Coromina, B. Adeniran, R. Mokaya and D. A. Walsh, *J. Mater. Chem. A*, 2016, **4**, 14586-14594.
4. P.-p. Chang, C.-y. Wang, T. Kinumoto, T. Tsumura, M.-m. Chen and M. Toyoda, *Carbon*, 2018, **131**, 184-192.
5. Y. An, Y. Yang, Z. Hu, B. Guo, X. Wang, X. Yang, Q. Zhang and H. Wu, *J. Power Sources*, 2017, **337**, 45-53.
6. Y. Lu, S. Zhang, J. Yin, C. Bai, J. Zhang, Y. Li, Y. Yang, Z. Ge, M. Zhang, L. Wei, M. Ma, Y. Ma and Y. Chen, *Carbon*, 2017, **124**, 64-71.
7. C. Li, X. Zhang, K. Wang, X. Sun, G. Liu, J. Li, H. Tian, J. Li and Y. Ma, *Adv. Mater.*, 2017, **29**, 1604690.
8. X. Liu, J. Guo, J. Chen, J. Zhang and J. Zhang, *J. Power Sources*, 2017, **363**, 54-60.
9. X. Wang, C. Lu, H. Peng, X. Zhang, Z. Wang and G. Wang, *J. Power Sources*, 2016, **324**, 188-198.
10. M. Karnan, K. Subramani, P. K. Srividhya and M. Sathish, *Electrochim. Acta*, 2017, **228**, 586-596.
11. J. K. Ewert, D. Weingarth, C. Denner, M. Friedrich, M. Zeiger, A. Schreiber, N. Jäckel, V. Presser and R. Kempe, *J. Mater. Chem. A*, 2015, **3**, 18906-18912.
12. H. Zhang, X. Zhang and Y. Ma, *Electrochim. Acta*, 2015, **184**, 347-355.
13. N. d. M. Pereira, J. P. C. Trigueiro, I. d. F. Monteiro, L. A. Montoro and G. G. Silva, *Electrochim. Acta*, 2018, **259**, 783-792.
14. M. Klose, R. Reinhold, K. Pinkert, M. Uhlemann, F. Wolke, J. Balach, T. Jaumann, U. Stoeck, J. Eckert and L. Giebeler, *Carbon*, 2016, **106**, 306-313.
15. B. Dyatkin, O. Gogotsi, B. Malinovskiy, Y. Zozulya, P. Simon and Y. Gogotsi, *J. Power Sources*, 2016, **306**, 32-41.
16. R. Sasi, S. Sarojam and S. J. Devaki, *ACS Sustainable Chem. Eng.*, 2016, **4**,

3535-3543.

17. D. Liu, C. Zeng, D. Qu, H. Tang, Y. Li, B.-L. Su and D. Qu, *J. Power Sources*, 2016, **321**, 143-154.
18. T. C. Mendes, C. Xiao, F. Zhou, H. Li, G. P. Knowles, M. Hilder, A. Somers, P. C. Howlett and D. R. MacFarlane, *ACS Appl. Mater. Interfaces*, 2016, **8**, 35243-35252.
19. L. Zhang, T. You, T. Zhou, X. Zhou and F. Xu, *ACS Appl. Mater. Interfaces*, 2016, **8**, 13918-13925.
20. Q. Shao, J. Tang, Y. Lin, J. Li, F. Qin, K. Zhang, J. Yuan and L.-C. Qin, *Electrochim. Acta*, 2015, **176**, 1441-1446.
21. Z. Qiu, Y. Lin, H. Xin, P. Han, D. Li, B. Yang, P. Li, S. Ullah, H. Fan, C. Zhu and J. Xu, *Carbon*, 2018, **126**, 85-92.
22. H. Huang, C. Cheng, S. Liang, C. Liang, Y. Xia, Y. Gan, J. Zhang, X. Tao and W. Zhang, *Carbon*, 2018, **130**, 559-565.
23. Y. Chen, L. Shi, S. Guo, Q. Yuan, X. Chen, J. Zhou and H. Song, *J. Mater. Chem. A*, 2017, **5**, 19866-19874.
24. D. Zhao, J. Zhang, C. Fu, J. Huang, D. Xiao, M. M. F. Yuen and C. Niu, *J. Mater. Chem. A*, 2018, **6**, 2540-2548.
25. H. Liu, Y. Tang, W. Zhao, W. Ding, J. Xu, C. Liang, Z. Zhang, T. Lin and F. Huang, *Adv. Mater. Interfaces*, 2018, **5**.
26. L. Shi, Y. Chen, G. Chen, Y. Wang, X. Chen and H. Song, *Carbon*, 2017, **123**, 186-192.
27. G. Zeng, B. Zhou, L. Yi, H. Li, X. Hu and Y. Li, *Sustainable Energy Fuels*, 2018, **2**, 855-861.
28. Y. Cui, H. Wang, X. Xu, Y. Lv, J. Shi, W. Liu, S. Chen and X. Wang, *Sustainable Energy Fuels*, 2018, **2**, 381-391.
29. Q. Xia, H. Yang, M. Wang, M. Yang, Q. Guo, L. Wan, H. Xia and Y. Yu, *Adv. Energy Mater.*, 2017, **7**, 1701336.
30. V. Selvamani, S. Gopi, V. Rajagopal, M. Kathiresan, S. Vembu, D. Velayutham and S. Gopukumar, *ACS Appl. Mater. Interfaces*, 2017, **9**, 39326-

39335.

31. H. Tao, L. Xiong, S. Du, Y. Zhang, X. Yang and L. Zhang, *Carbon*, 2017, **122**, 54-63.

32. S. Huang, Z. Li, B. Wang, J. Zhang, Z. Peng, R. Qi, J. Wang and Y. Zhao, *Adv. Funct. Mater.*, 2018, **28**, 1706294.

33. J. Chen, Z. Mao, L. Zhang, D. Wang, R. Xu, L. Bie and B. D. Fahlman, *ACS Nano*, 2017, **11**, 12650-12657.

34. D. Mhamane, M.-S. Kim, B.-H. Park, H.-S. Choi, Y. H. Kim, V. Aravindan, A. Phadkule and K.-B. Kim, *J. Mater. Chem. A*, 2018, **6**, 6422-6434.

35. Y. Wang, Y. Wang, J. Liu, L. Pan, W. Tian, M. Wu and J. Qiu, *Carbon*, 2017, **122**, 344-351.

36. X. Dong, H. Jin, R. Wang, J. Zhang, X. Feng, C. Yan, S. Chen, S. Wang, J. Wang and J. Lu, *Adv. Energy Mater.*, 2018, **8**, 1702695.

37. S. Zhu, K. Xu, S. Sui, J. Li, L. Ma, C. He, E. Liu, F. He, C. Shi, L. Miao, J. Jiang and N. Zhao, *J. Mater. Chem. A*, 2017, **5**, 19175-19183.

38. W. Yu, H. Wang, S. Liu, N. Mao, X. Liu, J. Shi, W. Liu, S. Chen and X. Wang, *J. Mater. Chem. A*, 2016, **4**, 5973-5983.

39. X. Zhou, F. Chen, T. Bai, B. Long, Q. Liao, Y. Ren and J. Yang, *Green Chem.*, 2016, **18**, 2078-2088.